CORRECTION OF DISTANCE-DEPENDENT BLURRING IN PROJECTION DATA FOR FULLY THREE-DIMENSIONAL ELECTRON MICROSCOPIC RECONSTRUCTION

Joanna Klukowska, Gabor T. Herman

Department of Computer Science
Graduate Center, City University of New York
New York, NY, USA

Ivan G. Kazantsev

Institute of Computational Mathematics
and Mathematical Geophysics,
Novosibirsk, Russia

ABSTRACT

We propose a method of correction for distance-dependent blurring, which is one of the limiting factors to achieving higher resolution in 3D reconstructions of biological specimens from 2D projections obtained by an electron microscope. Our proposed correction is based on the frequency-distance relation that has been used successfully in correction of a similar problem in single photon emission tomography and has been suggested for electron microscopy data obtained by rotating a sample around a single axis. We extend these approaches to electron microscopy data that are obtained from arbitrary directions. We develop the theoretical background for a correction method that results in an estimate of a true projection data set, which then can be used to obtain a 3D reconstruction by any currently existing algorithm.

Index Terms— distance-dependent blurring, contrast transfer function, electron microscopy, stationary phase

1. INTRODUCTION

Three-dimensional cryoelectron microscopy is a powerful tool for solving the structure of macromolecular complexes, providing resolution of order of a nanometer. The reconstruction techniques available these days turn the images obtained by an electron microscope (called *micrographs*) into three-dimensional models of biological structures as they exist in their native environment [1]. The models of the blurring that occurs in electron microscopes that are used by these reconstruction techniques are not completely accurate. Most models ignore the dependence of the blurring function on the distance from the electron source. This dependence is not important when the desired resolution is not great or when the specimen is small. As both the desired resolution of the final reconstructions and the size of the imaged specimens increase, the distance dependence can no longer be ignored.

The *point spread function* (PSF) is the response of an imaging system to an isolated point. In electron microscopy it is usually specified by its Fourier transform, which is referred to as the *contrast transfer function* (CTF). The CTF affects various frequencies by modulating the magnitude and by changing the sign of their amplitudes. In electron microscopy, the PSF is translation invariant within any plane perpendicular to the direction of electron beam, but changes from one such plane to the next. This is due to the dependence of defocus (one of the properties of an electron microscope encapsulated in the CTF) on the distance from the electron source. In micrographs the blurring caused by CTF has features both of smearing and size distortion ("zooming", deformation, etc.) that are dependent on the distance from the electron source. The size distortions are clearly visible in projection data in Fig. 1.

Several authors have approached this problem so far [2, 3, 4, 5, 6]. In the present work, we provide a fully three-dimensional generalization of the approach presented by Dubowy and Herman [5]. Our work is a generalization to 3D of the *frequency-distance relation* that was proposed for reconstruction of 2D activity distribution from 1D projections in SPECT [7]. Dubowy and Herman [5] developed an approach based on the principle of stationary phase that solves the problem of distance-dependent correction in the case of 2D projections obtained around a single axis of rotation. In this paper we propose generalization of this approach to 2D projections obtained from arbitrary directions.

2. MATHEMATICAL BACKGROUND AND NOTATION

Let X_1, X_2, and X_3 be coordinate axes of a Cartesian coordinate system attached to a microscope, with the X_3-axis parallel to an electron beam. Thus, projections are always taken parallel to the X_3-axis and it is the molecule that is rotated to obtain various projections.

Let $\mathbb{S} = [0, 2\pi) \times [0, \pi)$ be the set of directions in $\mathbb{R}^3$. For any $(\theta, \phi) \in \mathbb{S}$, we define the rotation matrices

$$D_\theta = \begin{pmatrix} \cos\theta & -\sin\theta & 0 \\ \sin\theta & \cos\theta & 0 \\ 0 & 0 & 1 \end{pmatrix}, \; D_\phi = \begin{pmatrix} \cos\phi & 0 & \sin\phi \\ 0 & 1 & 0 \\ -\sin\phi & 0 & \cos\phi \end{pmatrix}. \tag{1}$$

D_θ is a right-hand rotation by θ in the X_1X_2-plane and D_ϕ is a right-hand rotation by ϕ in the X_1X_3-plane. For shorter

and clearer notation we define

$$\left(x_1^F(\theta,\phi), x_2^F(\theta,\phi), x_3^F(\phi)\right)^T = D_\theta^{-1} D_\phi^{-1} (x_1, x_2, x_3)^T \tag{2}$$

and

$$\left(x_1^B(\theta,\phi), x_2^B(\theta), x_3^B(\theta,\phi)\right)^T = D_\phi D_\theta (x_1, x_2, x_3)^T. \tag{3}$$

The method of *stationary phase* [8, Chapter 1] is used for the evaluation of highly oscillatory integrals of the form

$$I(\xi) = \int_{c_1}^{c_2} G(\sigma)\, e^{i\xi F(\sigma)} d\sigma. \tag{4}$$

If G is a smooth function, F is twice differentiable, and all stationary points (points at which the second derivative of F is zero) of F are non-degenerate, then, as $\xi \to \infty$, the integral in (4) can be well approximated by a sum over the stationary points of F. It has been shown in many practical applications [5, 7, 9] that the sum approximates the original integral very well even for small values of ξ. In our work, the actual summation formula is not relevant. We simply make use of the fact that such an approximation is possible.

3. PROJECTION DATA

3.1. Blur-free projection data

Mathematically ideal projection data (data available from all directions and no noise) that would be generated by a blur-free electron microscope are modeled by

$$[\mathcal{P}v](\theta,\phi,x_1,x_2) = [\mathcal{C}\mathcal{R}v](\theta,\phi,x_1,x_2) \tag{5}$$

where $\mathcal{C}$ is an operator that integrates along the electron beam direction (X_3-axis) and $\mathcal{R}$ is an operator that, given a 3D function v and two angles, θ and ϕ, rotates v around the X_3-axis by θ and around the X_2-axis by ϕ. $\mathcal{C}$ and $\mathcal{R}$ are defined by

$$[\mathcal{C}w](\theta,\phi,x_1,x_2) = \int_{\mathbb{R}} w(\theta,\phi,x_1,x_2,x_3)\, dx_3, \tag{6}$$

$$[\mathcal{R}v](\theta,\phi,x_1,x_2,x_3) = v\left(x_1^F(\theta,\phi), x_2^F(\theta,\phi), x_3^F(\phi)\right). \tag{7}$$

3.2. Distance-dependently blurred projection data

3.2.1. Distance-dependent PSF

We denote by $h(x_1,x_2,x_3)$ the point spread function (PSF) of an electron microscope, and by $H(\xi_1,\xi_2,x_3)$ its Fourier transform in the first two variables, referred to as the contrast transfer function (CTF). The 2-dimensional Fourier transform of the PSF shifted perpendicularly to the X_3-axis to the point (x_1', x_2', x_3) can be computed using the *shift theorem* for Fourier transforms

$$\begin{aligned}\int_{\mathbb{R}^2} h(x_1 - x_1', x_2 - x_2', x_3)\, e^{-i(x_1\xi_1 + x_2\xi_2)} dx_1 dx_2 \\ = H(\xi_1,\xi_2,x_3)\, e^{-i\left(x_1'\xi_1 + x_2'\xi_2\right)}.\end{aligned} \tag{8}$$

3.2.2. Blurred projection data

The distance-dependently blurred projection data of v (still assuming data available from all directions and no noise) collected by an electron microscope can be modeled by

$$\mathcal{P}_h v = \mathcal{C}_h \mathcal{R} v, \tag{9}$$

where $\mathcal{C}_h$, defined by

$$C_h = \mathcal{C}[w * h], \tag{10}$$

is an operator that integrates along the X_3-axis the function that is the result of a convolution in x_1 and x_2 of w and h. The convolution step is a mathematical model of blurring that occurs during an imaging process.

3.3. Point object

Consider a case of imaging a "molecule" that is an impulse located at $(\widehat{x}_1, \widehat{x}_2, \widehat{x}_3)^T$. Let $\kappa(x_1,x_2,x_3) = \delta(\widehat{x}_1 - x_1)\, \delta(\widehat{x}_2 - x_2)\, \delta(\widehat{x}_3 - x_3)$. By (7) the rotated version of κ is

$$\begin{aligned}&[\mathcal{R}\kappa](x_1,x_2,x_3) \\ &= \delta\left(\widehat{x}_1 - x_1^F(\theta,\phi)\right) \delta\left(\widehat{x}_2 - x_2^F(\theta,\phi)\right) \delta\left(\widehat{x}_3 - x_3^F(\phi)\right).\end{aligned} \tag{11}$$

For this particular function though, it is equivalent to

$$\delta\left(\widehat{x}_1^B(\theta,\phi) - x_1\right) \delta\left(\widehat{x}_2^B(\theta) - x_2\right) \delta\left(\widehat{x}_3^B(\theta,\phi) - x_3\right). \tag{12}$$

We use the second of these expressions to represent the rotation of κ. The benefit of this will become clear soon.

The blur-free projection data $\mathcal{P}\kappa$ of our molecule κ is

$$[\mathcal{P}\kappa](\theta,\phi,x_1,x_2) = \delta\left(\widehat{x}_1^B(\theta,\phi) - x_1\right) \delta\left(\widehat{x}_2^B(\theta) - x_2\right), \tag{13}$$

as can be seen by applying (5) and (6) to (12). The 4D Fourier transform of $\mathcal{P}\kappa$ is

$$\begin{aligned}&[\mathcal{F}_4\mathcal{P}\kappa](\Theta,\Phi,\xi_1,\xi_2) \\ &= \frac{1}{(2\pi)^2} \int_0^{2\pi}\int_0^{\pi} e^{-i\left(\widehat{x}_1^B(\theta,\phi)\xi_1 + \phi\Phi\right)} d\phi\, e^{-i\left(\widehat{x}_2^B(\theta)\xi_2 + \theta\Theta\right)} d\theta.\end{aligned} \tag{14}$$

The distance-dependently blurred projection data of κ can be obtained by applying (9), (10) and two dimensional convolution in x_1 and x_2 to (12):

$$\begin{aligned}&[\mathcal{P}_h\kappa](\theta,\phi,x_1,x_2) \\ &= h\left(x_1 - \widehat{x}_1^B(\theta,\phi), x_2 - \widehat{x}_2^B(\theta), \widehat{x}_3^B(\theta,\phi)\right).\end{aligned} \tag{15}$$

The 4D Fourier transform of the distance-dependently blurred projection data of κ is

$$[\mathcal{F}_4\mathcal{P}_h\kappa](\Theta,\Phi,\xi_1,\xi_2) = \frac{1}{(2\pi)^2}\int_0^{2\pi}\int_0^{\pi} H(\xi_1,\xi_2,\widehat{x}_3(\theta,\phi)) \, e^{-i\left(\widehat{x}_1^B(\theta,\phi)\xi_1+\phi\Phi\right)}d\phi\, e^{-i\left(\widehat{x}_2^B(\theta)\xi_2+\theta\Theta\right)}d\theta. \tag{16}$$

3.4. Fourier analysis for the point object

We take a closer look now at the complex exponentials in (14) and (16). Following Xia, Lewitt and Edholm [7] and Dubowy and Herman [5], we apply the stationary phase method to the 4D Fourier transforms of blur-free (14) and distance-dependently blurred (16) projection data sets.

We first define a new function

$$f_{\theta,\Phi,\xi_1}(\phi) = \widehat{x}_1^B(\theta,\phi) + \phi\frac{\Phi}{\xi_1}. \tag{17}$$

We also need two other functions:

$$I^P_{\xi_1,\Phi}(\theta) = \int_0^{\pi} e^{-if_{\theta,\Phi,\xi_1}(\phi)\xi_1}d\phi, \tag{18}$$

$$I^{P_h}_{\xi_1,\xi_2,\Phi}(\theta) = \int_0^{\pi} H\left(\xi_1,\xi_2,\hat{x}_3^B(\theta,\phi)\right) e^{-if_{\theta,\Phi,\xi_1}(\phi)\xi_1}d\phi, \tag{19}$$

which are the inner integrals of (14) and (16). The integrals in (18) and (19) are highly oscillatory of the form of (4) and hence can be approximated using stationary phase theory. Noting from (1) and (3) that the partial derivative of $\widehat{x}_1^B(\theta,\phi)$ with respect to ϕ is $\hat{x}_3^B(\theta,\phi)$, we get that the stationary points $\tilde{\phi}$ of f_{θ,Φ,ξ_1} satisfy $f'_{\theta,\Phi,\xi_1}\left(\tilde{\phi}\right) = \widehat{x}_3^B\left(\theta,\tilde{\phi}\right) + \frac{\Phi}{\xi_1} = 0$. In other words, if S_{θ,Φ,ξ_1} is the (easily shown to be finite) set of stationary points of f_{θ,Φ,ξ_1}, then

$$S_{\theta,\Phi,\xi_1} = \left\{\tilde{\phi}\,|\,\widehat{x}_3^B\left(\theta,\tilde{\phi}\right) = -\frac{\Phi}{\xi_1}\right\}. \tag{20}$$

This is known as the *frequency-distance relation* and was discussed initially in the context of SPECT by Xia, Lewitt and Edholm [7] and then adapted to electron microscopy with single axis data collection mode by Dubowy and Herman [5].

The stationary phase approximation is valid only if the stationary points are non-degenerate; i.e., if the second derivative of f_{θ,Φ,ξ_1} is not zero at any stationary point $\tilde{\phi}$. This follows easily from (1) and (3) provided that $\widehat{x}_1^B\left(\theta,\tilde{\phi}\right) \neq 0$. The same equations also imply that the set T_{Φ,ξ_1} of θ for which $\widehat{x}_1^B\left(\theta,\tilde{\phi}\right) = 0$ for some $\tilde{\phi} \in S_{\theta,\Phi,\xi_1}$ is finite.

The important fact is that all stationary points of f_{θ,Φ,ξ_1} satisfy the same condition stated in (20). This means that we can use $H\left(\xi_1,\xi_2,-\frac{\Phi}{\xi_1}\right)$ in place of $H\left(\xi_1,\xi_2,\hat{x}_3^B(\theta,\phi_0)\right)$ and factor it out of the summation over stationary points that can be used to approximate the integral in (19). Since the integrals for $I^P_{\xi_1,\Phi}$ and $I^{P_h}_{\xi_1,\xi_2,\Phi}$ differ only in H, the approximation to (19) can be written as a product of the approximation of (18) and $H\left(\xi_1,\xi_2,-\frac{\Phi}{\xi_1}\right)$. This establishes the relationship between $I^P_{\xi_1,\Phi}$ and $I^{P_h}_{\xi_1,\xi_2,\Phi}$ as follows: For all $\theta \notin T_{\Phi,\xi_1}$,

$$I^{P_h}_{\xi_1,\xi_2,\Phi}(\theta) = H\left(\xi_1,\xi_2,-\frac{\Phi}{\xi_1}\right) I^P_{\xi_1,\Phi}(\theta). \tag{21}$$

The values of the outer integrals in (14) and (16) are not affected by the values of the inner integrals for the finitely many $\theta \in T_{\Phi,\xi_1}$. This implies that the 4D Fourier transform of the distance-dependently blurred projection data is related to the 4D Fourier transform of blur-free projection data:

$$[\mathcal{F}_4\mathcal{P}_h\kappa](\Theta,\Phi,\xi_1,\xi_2) \approx H\left(\xi_1,\xi_2,-\tfrac{\Phi}{\xi_1}\right)[\mathcal{F}_4\mathcal{P}\kappa](\Theta,\Phi,\xi_1,\xi_2). \tag{22}$$

4. CORRECTION OF THE PROJECTION DATA

The result in (22) based on the frequency-distance relation suggests a correction method for the Fourier coefficients of the distant-dependently blurred projection data in order to estimate the true projection data. The Fourier coefficients for the corrected projection data of v can be obtained by a division of the Fourier coefficients of the distance-dependently blurred projection data $P_h v$ by the CTF H; i.e., as

$$[\mathcal{F}_4\mathcal{P}_h v](\Theta,\Phi,\xi_1,\xi_2)\,/H\left(\xi_1,\xi_2,-\frac{\Phi}{\xi_1}\right). \tag{23}$$

At this step some regularization is required to avoid amplification of noise present in the data.

This is our final result. The advantage of correction in this fashion is that any of the large collection of reconstruction algorithms can be applied to the so-corrected data in the same way as is done currently with data corrected for the CTF that is appropriate only for a single layer of a specimen. The pipeline of reconstruction for 3D molecules from 2D projections needs to be simply amended by the new correction step, no other modifications are needed.

5. NUMERICAL RESULTS

We tested the correction method proposed in the previous section on a simple phantom composed of seven spheres digitized on a $128\times128\times128$ cubic voxel array. We computed the distance-dependently blurred projection data of that phantom

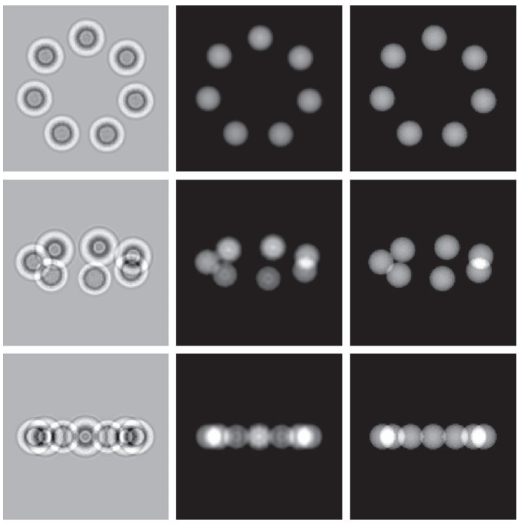

Fig. 1. Comparison of the distance-dependently blurred projections (first column) with the corrected projections (second column) and the ideal projections obtained with no blurring (third column) for three projection directions.

for 1600 directions. The set of micrographs was corrected according to (23). The results are presented in Fig. 1. Some blurring is still present in the corrected projections; this is due to having only a finite number of projection directions, the discrete Fourier transform implementation and numerical difficulties with (23) at places where the CTF is near zero.

The reconstruction obtained from the projections corrected by our method is illustrated in Fig. 2.

6. FUTURE WORK

Testing the results of the proposed correction method is the subject of our ongoing work. One technical difficulty in the implementation is the accurate computation of 4D Fourier transforms. The existence of spherical Fourier transform algorithms suggests that we will be able to overcome this. We plan to evaluate the proposed correction method on more complicated phantoms and in presence of noise.

The stationary phase approximation is mathematically justified only for high frequency coefficients. We plan to develop a weighting scheme that smoothly transitions between different methods of correction for high and low frequencies.

7. ACKNOWLEDGMENTS

Financial support by Award Number R01HL070472 from the National Heart, Lung, And Blood Institute is acknowledged. The content is solely the responsibility of the authors and does not represent the official views of the National Heart, Lung, And Blood Institute or the National Institutes of Health.

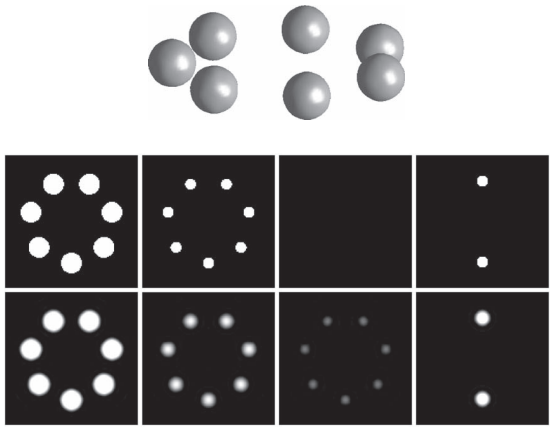

Fig. 2. Reconstruction from 1600 projections. Top: 3D rendering for voxel values thresholded at 0.5. Bottom: corresponding cross sections through the phantom (top row) and reconstruction (bottom row).

8. REFERENCES

[1] J. Frank, *Three-Dimensional Electron Microscopy of Macromolecular Assemblies*, Oxford Univ. Press, 2006.

[2] D.J. DeRosier, "Correction of high-resolution data for curvature of the Ewald sphere," *Ultramicroscopy*, vol. 81, pp. 83–98, 2000.

[3] G.J. Jensen and R.D. Kornberg, "Defocus-gradient corrected back-projection," *Ultramicroscopy*, vol. 84, pp. 57–64, 2000.

[4] Y. Wan, W. Chiu, and Z. H. Zhou, "Full contrast transfer function correction in 3D cryo-EM reconstruction," in *International Conference on Communications, Circuits and Systems*, 2004, pp. 960 – 964.

[5] J.N. Dubowy and G.T. Herman, "An approach to the correction of distance-dependent defocus in electron microscopic reconstruction," in *International Conference on Image Processing*, 2005, vol. 3, pp. 748–751.

[6] M. Wolf, D.J. DeRosier, and N. Grigorieff, "Ewald sphere correction for single-particle electron microscopy," *Ultramicroscopy*, vol. 106, pp. 376–82, 2006.

[7] W. Xia, R.M. Lewitt, and P.R. Edholm, "Fourier correction for spatially variant collimator blurring in SPECT," *IEEE Trans. Med. Im.*, vol. 14, pp. 100–115, 1995.

[8] V. Guillemin and S. Sternberg, *Geometric Asymptotics*, AMS, 1977.

[9] M. Defrise, "A factorization method for the 3D X-ray transform," *Inv. Prob.*, vol. 11, pp. 983–994, 1995.